

Electronic Control of Discrimination between O₂ and CO in Myoglobin Lacking the Distal Histidine Residue

Ryu Nishimura,[†] Tomokazu Shibata,[†] Izumi Ishigami,[‡] Takashi Ogura,[‡] Hulin Tai,[§] Satoshi Nagao,[§] Takashi Matsuo,[§] Shun Hirota,[§] Osami Shoji,^{||} Yoshihito Watanabe,^{||} Kiyohiro Imai,[⊥] Saburo Neya,[#] Akihiro Suzuki,[§] and Yasuhiko Yamamoto^{*,†}

[†]Department of Chemistry, University of Tsukuba, Tsukuba 305-8571, Japan

[‡]Department of Life Science, Graduate School of Life Science, University of Hyogo, Kamigori-cho, Ako-gun, Hyogo 678-1297, Japan

[§]Graduate School of Materials Science, Nara Institute of Science and Technology, Ikoma, Nara 630-0192, Japan

^{||}Department of Chemistry, Graduate School of Science, Nagoya University, Furo-cho, Chikusa-ku, Nagoya 464-8602, Japan

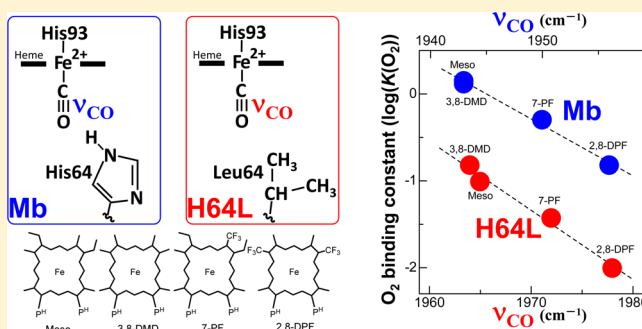
[⊥]Department of Frontier Bioscience, Faculty of Bioscience and Applied Chemistry, Hosei University, Koganei, Tokyo 184-8584, Japan

[#]Department of Physical Chemistry, Graduate School of Pharmaceutical Sciences, Chiba University, Chuoh-Inohana, Chiba 260-8675, Japan

[§]Department of Materials Engineering, Nagaoka National College of Technology, Nagaoka 940-8532, Japan

Supporting Information

ABSTRACT: We analyzed the oxygen (O₂) and carbon monoxide (CO) binding properties of the H64L mutant of myoglobin reconstituted with chemically modified heme cofactors possessing a heme Fe atom with a variety of electron densities, in order to elucidate the effect of the removal of the distal His64 on the control of both the O₂ affinity and discrimination between O₂ and CO of the protein by the intrinsic heme Fe reactivity through the electron density of the heme Fe atom (ρ_{Fe}). The study revealed that, as in the case of the native protein, the O₂ affinity of the H64L mutant protein is regulated by the ρ_{Fe} value in such a manner that the O₂ affinity of the protein decreases, due to an increase in the O₂ dissociation rate constant, with a decrease in the ρ_{Fe} value, and that the O₂ affinities of the mutant and native proteins are affected comparably by a given change in the ρ_{Fe} value. On the other hand, the CO affinity of the H64L mutant protein was found to increase, due to a decrease in the CO dissociation rate constant, with a decrease in the ρ_{Fe} value, whereas that of the native protein was essentially independent of a change in the ρ_{Fe} value. As a result, the regulation of the O₂/CO discrimination in the protein through the ρ_{Fe} value is affected by the distal His64. Thus, the study revealed that the electronic tuning of the intrinsic heme Fe reactivity through the ρ_{Fe} value plays a vital role in the regulation of the protein function, as the heme environment furnished by the distal His64 does.



INTRODUCTION

Myoglobin (Mb), an oxygen storage hemoprotein, is one of the most thoroughly studied proteins and has been used as a paradigm for the structure–function relationships of metalloproteins.^{1–9} Dioxygen (O₂) and also carbon monoxide (CO) are reversibly bound to a ferrous heme Fe atom (Fe(II)) in Mb. As a respiratory protein, Mb must favor the binding of O₂ in comparison to the toxic ligand CO ubiquitously produced from a variety of sources in biological systems.² The abilities of Mb to stabilize Fe(II)-bound O₂ and to discriminate against CO binding are usually evaluated on the basis of the *M* value: i.e., the ratio between the equilibrium constants for CO and O₂ binding ($K(\text{CO})/K(\text{O}_2)$).⁶ The *M* value was reported to be $\sim 2 \times 10^4$ for unencumbered model heme Fe(II) complexes in

organic solvents,^{8,10} and such a strong preference of heme Fe(II) for CO binding inhibits the O₂ storage function of the protein.

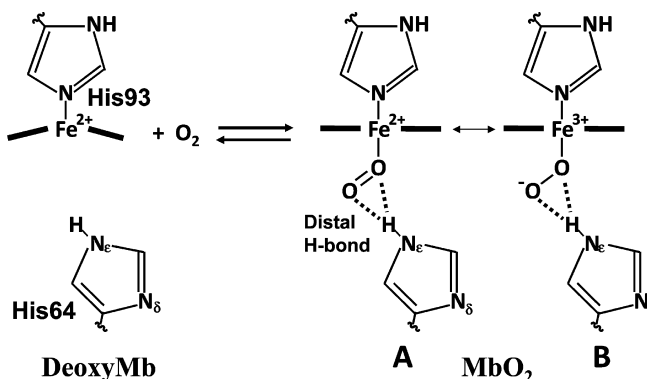
The regulation of the Mb function has been shown to be achieved through the heme environment furnished by nearby amino acid residues^{6–9} and electronic tuning of the intrinsic heme Fe reactivity.^{11–13} The heme environmental effects on the protein function have been elucidated in some detail, and in particular, it is well-known that the distal His (His64) contributes significantly by increasing the O₂ affinity of the protein by stabilizing Fe(II)-bound O₂ through a hydrogen-

Received: October 17, 2013

Published: December 30, 2013

bonding interaction between the His64 N_εH proton and the bound O₂ (distal H bond) (Scheme 1).^{1,14–16} Recently, we

Scheme 1. Oxygenation of Deoxy Mb^a



^aThe binding of O₂ to the heme Fe is stabilized by the hydrogen bonding between the Fe(II)-bound O₂ and His64 (distal H-bond).^{1,14,16} Structure (B) of the oxy form is only a proposed one.^{20,21}

found that both the O₂ affinity and CO/O₂ discrimination of the protein are regulated by the intrinsic heme Fe reactivity through the heme electronic structure.¹¹ In order to elucidate the electronic mechanism responsible for control of the Mb function, we have constructed a unique system composed of Mbs reconstituted with designed artificial heme cofactors such as mesoheme (Meso), 3,8-dimethyldeuteroporphyrinatoiron(III)^{17,18} (3,8-DMD), 13,17-bis(2-carboxylatoethyl)-3,8-diethyl-2,12,18-trimethyl-7-trifluoromethylporphyrinatoiron(III)¹⁹ (7-PF), and 13,17-bis(2-carboxylatoethyl)-3,7-diethyl-12,18-trimethyl-2,8-ditrifluoromethylporphyrinatoiron(III)¹¹ (2,8-DPF); i.e., Mb(Meso), Mb(3,8-DMD), Mb(7-PF), and Mb(2,8-DPF), respectively. These heme cofactors differ in the numbers of CF₃, CH₃, and C₂H₅ side chains (Figure 1). The substitution of strongly electron withdrawing trifluoromethyl (CF₃) group(s), as side chain(s) of heme cofactors, causes large and stepwise alterations of the heme electronic structure, and since 7-PF and 2,8-DPF can be considered as counterparts of Meso and 3,8-DMD, respectively, the functional consequences of the substitution of one and two CF₃ groups can be elucidated from the results of comparative studies on Mb(Meso) and Mb(7-PF), and Mb(3,8-DMD) and Mb(2,8-DPF), respectively. Through studies on the reconstituted protein system,¹¹ we revealed that the control of the *M* value is achieved through the effect of a change in the electron density of the heme Fe atom (ρ_{Fe}) on the O₂ affinity, which can be

reasonably interpreted in terms of the effect of a change in the ρ_{Fe} value on the resonance process between the Fe²⁺–O₂ and Fe³⁺–O₂[–]-like species^{20,21} (Scheme 1). On the other hand, in contrast to O₂ binding, the CO affinity of the protein was shown to be almost independent of the ρ_{Fe} value.¹¹

In this study, we elucidated the effect of the removal of the distal His64, and hence the distal H bond, on the control of the intrinsic heme Fe reactivity through the ρ_{Fe} value. In order to achieve this, we characterized the O₂ and CO binding properties of the H64L mutant⁶ (H64L(Proto)) and the mutant protein reconstituted with Meso, 3,8-DMD, 7-PF, and 2,8-DPF, i.e., H64L(Meso), H64L(3,8-DMD), H64L(7-PF), and H64L(2,8-DPF), respectively, and then the results for the mutant proteins were compared with those for the native proteins. H64L(Proto) has been investigated exhaustively as a typical Mb mutant protein to reveal the functional and structural consequences of the removal of the distal His64,^{6,22–27} and hence we could take advantage of the detailed functional and structural properties reported for the mutant protein.^{6,22–27} The study demonstrated that the differences in the ρ_{Fe} values of the H64L mutant proteins are clearly reflected in the stretching frequencies of the Fe-bound CO (ν_{CO}) in the CO forms of the mutant proteins, as has been reported for the native proteins,¹³ and that the O₂ affinities, i.e., *K*(O₂) values, of the mutant proteins correlated well with the ν_{CO} values. The plots of the quantity $\log(K(\text{O}_2))$ against the ν_{CO} values ($\log(K(\text{O}_2))$ – ν_{CO} plots) for the mutant proteins could be represented by a straight line, and the slope of the $\log(K(\text{O}_2))$ – ν_{CO} plots of the mutant proteins was identical with that of similar plots previously reported for the native proteins.¹¹ These results demonstrated not only that the electronic control of the O₂ affinity of Mb through the ρ_{Fe} value is not affected by the removal of the distal His64 but also that the regulation of the O₂ affinity through the heme environment furnished by the His64^{1,6,27} and that of electronic tuning of the intrinsic heme Fe reactivity through the ρ_{Fe} value are independent of each other. In contrast to O₂ binding, the effects of a change in the ρ_{Fe} value on the CO binding properties were found to differ between the H64L mutant and native proteins in such a manner that the CO affinity of the mutant protein increased with decreasing ρ_{Fe} value, while that of the native protein was essentially independent of the ρ_{Fe} value. As a result, the *M* value of the H64L mutant protein was more greatly affected by a given change in the ρ_{Fe} value than that of the native protein.

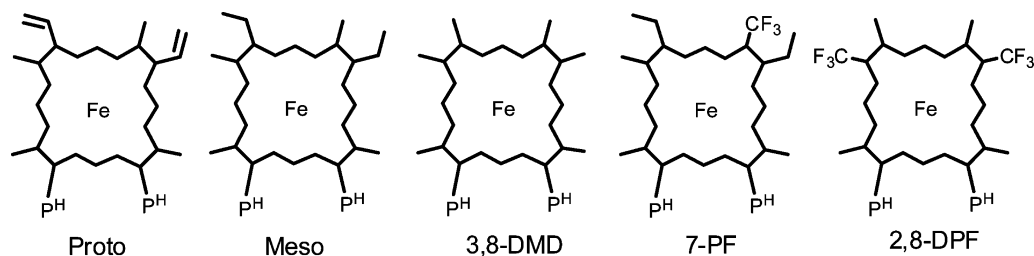


Figure 1. Schematic representation of the structures of the heme cofactors used in this study: i.e., protoheme (Proto), mesoheme (Meso), 3,8-dimethyldeuteroporphyrinatoiron(III)^{17,18} (3,8-DMD), 13,17-bis(2-carboxylatoethyl)-3,8-diethyl-2,12,18-trimethyl-7-trifluoromethylporphyrinatoiron(III)¹⁹ (7-PF), and 13,17-bis(2-carboxylatoethyl)-3,7-diethyl-12,18-trimethyl-2,8-ditrifluoromethylporphyrinatoiron(III)¹¹ (2,8-DPF). P^H represents –CH₂CH₂COOH.

MATERIALS AND METHODS

Materials and Protein Samples. All reagents and chemicals were obtained from commercial sources and used as received. Sperm whale Mb was purchased as a lyophilized powder from Biozyme and used without further purification. The expression and purification of the H64L mutant (H64L(Proto)) were carried out according to the methods described by Springer et al.⁶ Meso-heme (Meso) was purchased from Frontier Scientific Co. 3,8-DMD,^{17,18} 7-PF,¹⁹ and 2,8-DPF¹¹ were synthesized as previously described. The apoproteins of H64L(Proto) and native protein (Mb(Proto)) were prepared at 4 °C according to the procedure of Teale,²⁸ and reconstituted H64L mutant and native proteins were prepared by slow addition of a synthetic heme cofactor to the corresponding apoproteins in 50 mM potassium phosphate buffer, pH 7.0, at 4 °C.¹¹ In order to prepare the CO and O₂ forms of the H64L mutant and native proteins, the proteins were reduced by adding Na₂S₂O₄ (Nakalai Chemicals Ltd.) in the presence of CO gas (Japan Air Gases) and in the air, respectively. Excess agent was removed by passage through a Sephadex G-10 (Sigma-Aldrich Co.) column equilibrated with an appropriate buffer solution. The met-cyano forms of the H64L mutant proteins, i.e., H64LCN, were prepared by adding KCN (Nakalai Chemicals Ltd.) to the met forms of the proteins obtained through oxidation of the proteins using K₃Fe(CN)₆ (Nakalai Chemicals Ltd.). The pH of each sample was measured with a Horiba F-22 pH meter equipped with a Horiba type 6069-10c electrode. The pH of a sample was adjusted using 0.1 M NaOH or HCl.

NMR Spectroscopy. ¹H spectra of H64LCNs were recorded on a Bruker AVANCE-400 spectrometer operating at the ¹H frequency of 400 MHz. Typical ¹H NMR spectra consisted of about 20k transients with a 100 kHz spectral width and 16k data points. The signal to noise ratio of the spectra was improved by apodization, which introduced ~10 Hz line broadening. The chemical shifts of ¹H NMR spectra are given in ppm downfield from the residual ¹H₂O peak at 4.75 ppm, as a secondary reference.

Oxygen Equilibrium Curves. Oxygen equilibrium curves (OECs) for the H64L mutant proteins were measured with 30 μM protein in 100 mM phosphate buffer, pH 7.4, and 100 mM Cl⁻ at 20 °C, using the previously described automatic recording apparatus.²⁹ P₅₀ values were determined through nonlinear least-squares fitting of the OEC data.³⁰

Kinetic Measurements of O₂ and CO Binding. Kinetic measurements of O₂ and CO binding of the H64L mutant proteins were carried out in 100 mM phosphate buffer, pH 7.40, at 20 °C, by means of the ligand displacement methods described previously.^{31–35} Flash photolysis using a 5 ns pulse Nd:YAG laser (532 nm) was performed on the CO forms of the H64L mutant proteins (H64LCOs) in the presence of a gas mixture of O₂ and CO in a ratio of 35:65. The rate constants for O₂ association ($k_{\text{on}}(\text{O}_2)$) and the pseudo-first-order rate constants for O₂ dissociation ($k_{\text{off}}(\text{O}_2)$) of H64L(Meso), H64L(3,8-DMD), H64L(7-PF), H64L(2,8-DPF), and H64L(Proto) were determined through analysis of the time evolution of the absorbance at the optimized wavelength for each protein sample, after the photolysis, which exhibited biphasic behavior, and the fast and slow phases with time scales of approximately microseconds and milliseconds, respectively, represent O₂ binding: i.e., $k_{\text{on}}(\text{O}_2)$, and the displacement of transiently bound O₂ by the CO present in the sample solution, i.e., $k_{\text{off}}(\text{O}_2)$, respectively. The equilibrium constants for O₂ binding ($K(\text{O}_2)$) were calculated from the kinetic data, i.e., the $k_{\text{on}}(\text{O}_2)$ and $k_{\text{off}}(\text{O}_2)$ values.

The rate constants for CO association ($k_{\text{on}}(\text{CO})$) of the mutant proteins were measured through analysis of the time evolution of the absorbance at 410, 410, 410, 416, and 424 nm, respectively, after photolysis of the CO forms under 1 atm of CO: i.e., CO concentration ([CO]) 9.85×10^{-4} M. The $k_{\text{on}}(\text{CO})$ value can be determined from the observed pseudo-first-order rate constant for CO association ($k_{\text{obs}}(\text{CO})$) using the equation $k_{\text{obs}}(\text{CO}) \approx k_{\text{on}}(\text{CO})$, because the rate constant of CO dissociation ($k_{\text{off}}(\text{CO})$) is $\ll k_{\text{on}}(\text{CO}) \times [\text{CO}]$. Then, the $k_{\text{off}}(\text{CO})$ value was determined by analysis of the displacement of Fe-bound CO and the oxidation of heme Fe by K₃Fe(CN)₆.^{33–35}

Similarly to the case of the study on O₂ binding, the equilibrium constants for CO binding ($K(\text{CO})$) were calculated from the kinetic data: i.e., the $k_{\text{on}}(\text{CO})$ and $k_{\text{off}}(\text{CO})$ values.

Resonance Raman Spectroscopy. Resonance Raman scattering was performed with excitation at 413.1 nm with a Kr⁺ laser (Spectra Physics, BeamLok 2060), dispersed with a polychromator (SPEX 1877, 1200 grooves/mm grating) and detected with a liquid-nitrogen-cooled charge coupled device (CCD) detector (CCD-1024 × 256-OPEN-1LS; HORIBA Jobin Yvon).³⁶ The protein concentrations were approximately 40 μM in 100 mM potassium phosphate buffer, pH 7.4. For measurements of the O₂ forms of the H64L mutant proteins (H64LO₂s), the protein samples were kept cool in order to inhibit autooxidation of the proteins. Raman shifts were calibrated with indene as a frequency standard. The positions of the bands were determined through fitting with Voigt profiles, which are convolutions of Gaussian and Lorentzian functions,³⁷ and the accuracy of the peak positions of well-defined Raman bands was $\pm 1 \text{ cm}^{-1}$.

RESULTS

¹H NMR Spectra of Met-cyano Forms of the H64L Mutant Proteins. ¹H NMR spectra (400 MHz) of H64LCN-(Meso), H64LCN(3,8-DMD), H64LCN(7-PF), H64LCN(2,8-DPF), and H64LCN(Proto) are shown in Figure 2. The

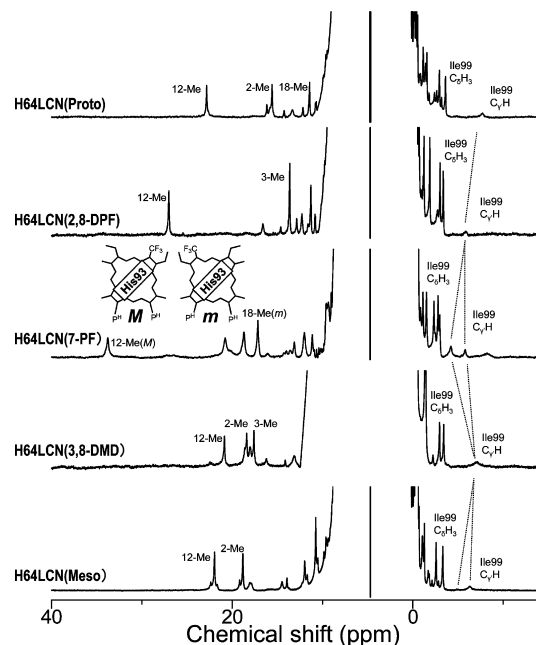


Figure 2. 400 MHz ¹H NMR spectra of H64LCN(Meso), H64LCN(3,8-DMD), H64LCN(7-PF), H64LCN(2,8-DPF), and H64LCN(Proto) at pH 7.40 in 90% H₂O/10% ²H₂O at 25 °C. The assignments of Ile99^{41,42} proton signals and the tentative ones of heme methyl proton signals are given with the spectra, and the M and m forms in the inset represent the two different orientations of 7-PF, relative to the protein.⁴³ The Ile99 C_γH proton signals of the mutant proteins are connected by a broken line.

paramagnetically shifted NMR signals due to heme side chain protons and amino acid protons in close proximity to the heme in a protein are well-resolved from the so-called diamagnetic envelope where protein proton signals overlap severely and have been shown to be quite sensitive to the heme electronic structure and the heme active site structure, respectively.^{38–40} The shift patterns of the paramagnetically shifted ¹H NMR signals of the H64L mutant proteins were similar to those of the native proteins possessing identical heme cofactors (Figure

Table 1. O₂ and CO Binding Parameters for H64Ls and Mbs at pH 7.40 and 25 °C

heme	protein	O ₂ binding				CO binding			
		$k_{\text{on}}(\text{O}_2)$ (mM ⁻¹ s ⁻¹)	$k_{\text{off}}(\text{O}_2)$ (s ⁻¹)	$K(\text{O}_2)$ (μM ⁻¹)	P_{50}^c (mmHg)	$k_{\text{on}}(\text{CO})$ (μM ⁻¹ s ⁻¹)	$k_{\text{off}}(\text{CO})$ (s ⁻¹)	$K(\text{CO})$ (μM ⁻¹)	M ($K(\text{CO})/K(\text{O}_2)$)
Meso	H64L	222 ± 66.6	2300 ± 970	0.097 ± 0.069	n.d. ^d	28.9 ± 8.7	0.25 ± 0.075	116 ± 48.7	1200 ± 66.6
	Mb ^a	8.2 ± 1.6	5.7 ± 1.1	1.5 ± 0.4	0.38	0.38 ± 0.07	0.048 ± 0.009	7.9 ± 2.4	5.5 ± 2.2
3,8-DMD	H64L	292 ± 87.6	1900 ± 800	0.15 ± 0.11	~10 ^e	31.9 ± 9.6	0.23 ± 0.069	139 ± 58.4	930 ± 87.6
	Mb ^b	12 ± 2	9.7 ± 1.9	1.3 ± 0.3	0.50	0.16 ± 0.03	0.024 ± 0.005	6.7 ± 2.0	5.1 ± 2.0
7-PF	H64L	212 ± 63.6	5700 ± 2400	0.037 ± 0.026	54	21.1 ± 6.3 ^f	0.052 ± 0.016	580 ± 244	11000 ± 63.6
	Mb ^a	12 ± 2	17 ± 3	0.5 ± 0.1	1.10	0.32 ± 0.06	0.032 ± 0.006	10 ± 3	21 ± 8
2,8-DPF	H64L	305 ± 91.5	31000 ± 13000	0.0098 ± 0.007	97	29.0 ± 8.7	0.053 ± 0.016	547 ± 230	56000 ± 91.5
	Mb ^a	8.3 ± 1.6	110 ± 22	0.15 ± 0.03	2.80	0.69 ± 0.14	0.036 ± 0.007	19 ± 6	132 ± 53
Proto	H64L	228 ± 68.4	3200 ± 1300	0.071 ± 0.05	14	30.0 ± 9.0	0.061 ± 0.018	492 ± 207	6900 ± 68.4
	Mb ^a	14 ± 3	12 ± 2	1.2 ± 0.3	0.58	0.51 ± 0.06	0.019 ± 0.005	27 ± 8	23 ± 9

^aTaken from ref 11. ^bTaken from ref 13. ^cDetermined from the oxygen equilibrium curve at pH 7.40 and 20 °C. ^dNot determined due to fast autoxidation. ^eAccurate determination of the value was hampered by fast autoxidation. ^fThe biphasic time course of CO association was fitted by the sum of two exponentials, and the value closer to those of the other H64L mutant proteins is indicated, the other one being 5.69 ± 1.7.

2; see also Figure S1 in the Supporting Information), indicating that the heme cofactors of the mutant proteins were accommodated properly, as those in the native proteins were. Furthermore, similarity in the shifts of Ile99 C_βH₃ and C_δH₃ proton signals, resolved at ~-4 ppm,^{41,42} among not only the mutant but also the native proteins, supported that the orientations of the heme cofactors with respect to the polypeptide chains in these mutant proteins are similar to those in the native proteins. In addition, the observation of two sets of heme methyl proton signals in the spectra of H64LCN(Meso) and H64LCN(7-PF), the ratios being 9:1 and 1:2.2 for the major (*M*) and minor forms (*m*), respectively, is due to the presence of well-known heme orientational isomers,⁴³ as depicted in the inset in Figure 2.

Effects of Heme Modifications on Functional Properties of the H64L Mutant Proteins. The $k_{\text{on}}(\text{O}_2)$, $k_{\text{off}}(\text{O}_2)$, $K(\text{O}_2)$, $k_{\text{on}}(\text{CO})$, $k_{\text{off}}(\text{CO})$, $K(\text{CO})$, and P_{50} values, together with the *M* values, of the H64L mutant proteins possessing various heme cofactors are summarized in Table 1. The time course of CO association of H64L(7-PF) was better fitted by the sum of two exponentials, and a $k_{\text{on}}(\text{CO})$ value close to those of the other H64L mutant proteins is indicated. The P_{50} values of H64L(Meso) and H64L(3,8-DMD) could not be determined accurately due to their rapid autoxidation. The kinetic parameters of O₂ and CO binding of H64L(Proto) were similar to the corresponding parameters reported by Rohlfs et al.³² As was demonstrated previously,³² the $k_{\text{on}}(\text{O}_2)$ and $k_{\text{on}}(\text{CO})$ values of Mb(Proto) were increased by factors of ~20 and ~60, respectively, by the H64L mutation, leading to a considerable decrease in the O₂ affinity. In contrast, the CO affinity of Mb(Proto) was largely increased by the mutation, because the $k_{\text{off}}(\text{O}_2)$ and $k_{\text{off}}(\text{CO})$ values of H64L(Proto) were larger by factors of ~300 and ~3, respectively, relative to the corresponding values of Mb(Proto) (Table 1). The increases in the $k_{\text{on}}(\text{O}_2)$ and $k_{\text{on}}(\text{CO})$ values induced by the mutation have been attributed, in part, to the absence of water molecules in the heme pocket,²² which have to be displaced before binding of exogenous ligands. In addition, as expected from structural consequence of the H64L mutation, the dramatic increase in the $k_{\text{off}}(\text{O}_2)$ value induced by the mutation is due to the absence of the distal H bond.^{1,32} A large difference in the *M* value between Mb(Proto) and H64L(Proto), i.e., 23 ± 9 and 6900 ± 5700, respectively (Table 1), clearly indicated a

significant contribution of the distal H bond to the regulation of the CO/O₂ discrimination in the protein.^{1,6,32}

Comparison of the O₂ binding parameters among the mutant proteins possessing various heme cofactors revealed that the $k_{\text{off}}(\text{O}_2)$ value increases steadily with increasing number of CF₃ substitutions, whereas the $k_{\text{on}}(\text{O}_2)$ value is affected only slightly by CF₃ substitutions. Consequently, the decreases in the O₂ affinity of the H64L mutant protein induced by CF₃ substitutions is due solely to increases in the $k_{\text{off}}(\text{O}_2)$ value. Hence, the effects of a change in the ρ_{Fe} value on the O₂ binding properties of the mutant protein were qualitatively similar to those of the native protein.^{11,13} On the other hand, the effects of a change in the ρ_{Fe} value on the CO binding properties of the mutant protein were somewhat different from the case of the native value. Although both the $k_{\text{on}}(\text{CO})$ and $k_{\text{off}}(\text{CO})$ values of the native protein were essentially independent of a change in the ρ_{Fe} value,^{11,13} the $k_{\text{off}}(\text{CO})$ value of the mutant protein was decreased by the CF₃ substitutions, whereas its $k_{\text{on}}(\text{CO})$ value was not greatly affected, leading to an increase in the CO affinity of the mutant protein induced by the CF₃ substitutions. As a result, as reflected in the *M* value, the CO/O₂ discrimination in the mutant protein is enhanced remarkably with decreasing ρ_{Fe} value (Table 1): i.e., the *M* value increased by a factor of ~9 on the substitution of one CF₃ group, as demonstrated for the H64L(Meso)/H64L(7-PF) system, and then by a factor of ~60 on the substitution of two CF₃ groups, as revealed on analysis of the H64L(3,8-DMD)/H64L(2,8-DPF) system.

Vibrational Frequencies of Fe-Bound CO of the H64L Mutant Proteins. The stretching frequency of Fe-bound CO (ν_{CO}) and the Fe–C stretching (ν_{FeC}) and Fe–C–O bending frequencies (δ_{FeCO}) in the mutant proteins possessing various heme cofactors were determined using resonance Raman spectroscopy. The mutant protein exhibited a single ν_{CO} band, as shown in Figure 3, which is in sharp contrast to the case of the native protein exhibiting a ν_{CO} band composed of multiple components, possibly due to the presence of multiple conformational states of the Fe–CO fragment (see Figure S2 in the Supporting Information).¹³ This finding demonstrated the significant effect of the conformational properties of the His64 side chain on the ν_{CO} band of the protein.^{23–25} In contrast, as also observed for the native proteins,¹³ the ν_{FeC} and δ_{FeCO} bands of the mutant proteins were each observed as a single component. The determined ν_{CO} , ν_{FeC} , and δ_{FeCO} bands of the

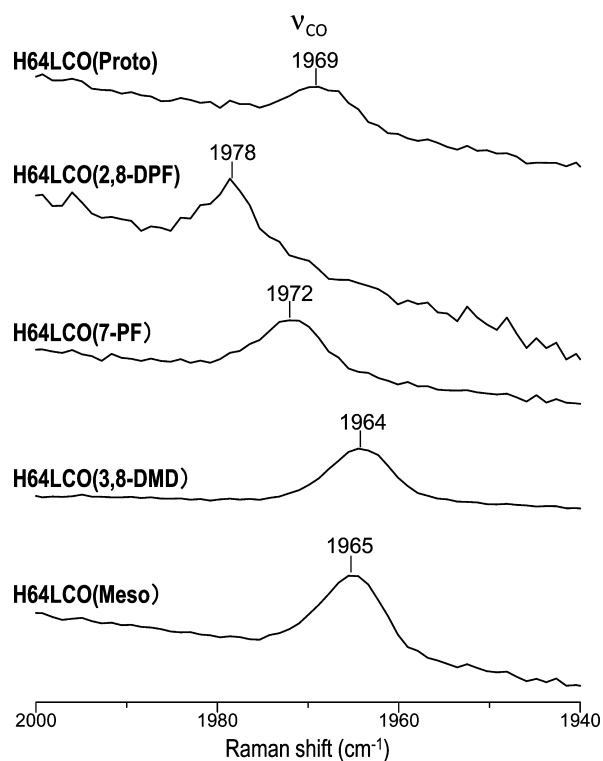
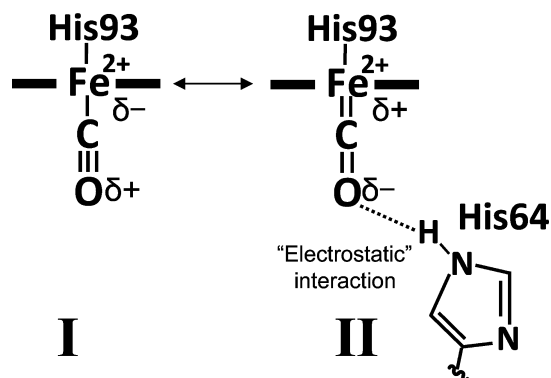


Figure 3. High-frequency regions of visible resonance Raman spectra of H64LCO(Meso), H64LCO(3,8-DMD), H64LCO(7-PF), H64LCO(2,8-DPF), and H64LCO(Proto) at pH 7.40 and 25 °C. The positions of the individual component ν_{CO} bands of the proteins determined through fitting with Voigt profiles³⁷ are indicated with the spectra.

mutant proteins are given in Table 2. The ν_{CO} , ν_{FeC} , and δ_{FeCO} values of H64LCO(Proto) were determined to be 1969, 491, and 574 cm^{-1} , respectively, these values being similar to the corresponding values previously reported by Anderton et al.²⁵ i.e., 1966, 489, and 573 cm^{-1} , respectively.

As shown in Table 2, the ν_{CO} and ν_{FeC} values of H64LCO(Proto) were larger and smaller, respectively, by $\sim 20 \text{ cm}^{-1}$ relative to the corresponding ones of MbCO(Proto), whereas the δ_{FeCO} one was affected only slightly by the mutation. A reciprocal relationship between the ν_{CO} and ν_{FeC} values has been reported for a variety of hemoproteins and has been interpreted in terms of an admixture of two alternative canonical forms of the Fe–CO fragment illustrated in Scheme 2.^{44,45} Hence, the changes of the ν_{CO} and ν_{FeC} values due to the H64L mutation have been attributed to the effect of the

Scheme 2. Resonance between the Two Canonical Forms of the Fe–CO Fragment, Represented by the Valence Bond Formalism^{a,44,45}



^aThe larger the ρ_{Fe} value, the better the heme Fe atom can serve as a π donor to CO. The stronger the Fe–CO bond, the larger the bond order of the Fe–CO bond, the smaller the C–O bond order, and hence the weaker the C–O bond. The distal His64 provides a positive electrostatic potential near the O atom of the Fe-bound CO and hence contributes to stabilization of $\text{Fe}^{2+(\delta^+)}\text{--CO}^{\delta^-}$.

removal of the electrostatic field exerted by the His64 side chain on the resonance of the Fe–CO fragment.

Comparison of the determined values among the mutant proteins revealed that the ν_{CO} , ν_{FeC} , and δ_{FeCO} values were all affected by the heme cofactor modifications. In particular, as in the case of the native protein,¹³ the ν_{CO} value increased dramatically with the CF_3 substitutions (Table 2). Comparison of the ν_{CO} values of the mutant proteins yielded a difference of 7 cm^{-1} for the H64L(Meso)/H64L(7-PF) system, which is half the value (14 cm^{-1}) for the H64L(3,8-DMD)/H64L(2,8-DPF) system. These results demonstrated the additive effect of the heme π system perturbation on the ν_{CO} value for the mutant proteins, as reported previously for the native proteins.^{13,46} In addition, the ν_{CO} values of the mutant proteins were larger by 21–22 cm^{-1} relative to the high-frequency ν_{CO} values ($\nu_{\text{CO(H)}}$), i.e., the position of the highest-frequency band among the multiple ν_{CO} band components¹³ (see Figure S3 in the Supporting Information), of the native proteins possessing identical heme cofactors. These results indicated that the effect of the H64L mutation on the ν_{CO} value is essentially independent of the heme cofactor. On the other hand, the ν_{FeC} values of the mutant proteins were smaller by 21–28 cm^{-1} relative to those of the native proteins possessing identical heme cofactors. Comparison of the ν_{FeC} values of the mutant proteins yielded differences of 1 and 11 cm^{-1} for the

Table 2. Vibrational Frequencies of the Fe-Bound CO of H64LCOs and MbCOs and the Fe-Bound O_2 of H64LO₂s and MbO₂s at pH 7.40 and 25 °C

	ν_{CO}^a (cm^{-1})		ν_{FeC}^b (cm^{-1})		δ_{FeCO}^c (cm^{-1})		ν_{FeO}^d (cm^{-1})	
	H64L	Mb ^e	H64L	Mb ^a	H64L	Mb ^a	H64L	Mb
Meso	1965	1943 ^f	489	515	575	576	573	573
3,8-DMD	1964	1943 ^f	491	514	575	576	570	571
7-PF	1972	1950 ^f	489	514	573	575	568	571
2,8-DPF	1978	1956 ^f	483	512	570	574	568	569
Proto	1969	1947 ^f	490	512	574	576	569	571

^aThe C–O stretching frequency of the Fe-bound CO. ^bThe Fe–C stretching frequency of the Fe-bound CO. ^cThe Fe–C–O bending frequency of the Fe-bound CO. ^dThe Fe–O stretching frequency of the Fe-bound O_2 . ^eTaken from ref 13. ^f $\nu_{\text{CO(H)}}$ (see Figure S3 in the Supporting Information), taken from ref 13.

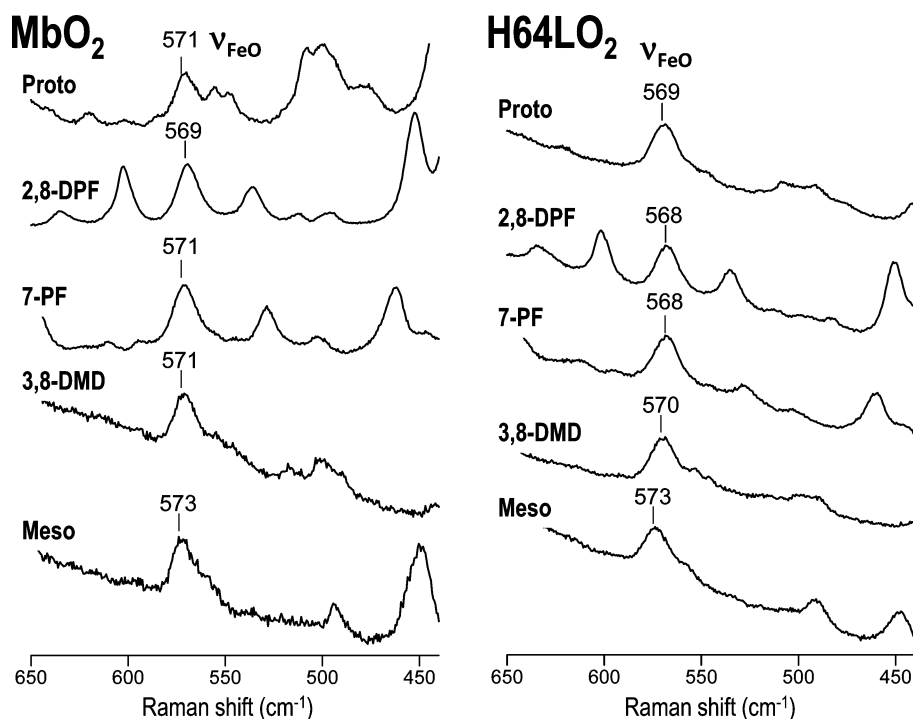


Figure 4. Visible resonance Raman spectra of MbO₂s (left) and H64LO₂s (right) at pH 7.40 and 25 °C. The positions of the ν_{FeO} bands of the proteins determined through fitting with Voigt profiles³⁷ are indicated with the spectra.

H64L(Meso)/H64L(7-PF) and H64L(3,8-DMD)/H64L(2,8-DPF) systems, respectively. Hence, in contrast to the case of the ν_{CO} value, an additive effect of the heme π system perturbation was not observed for the ν_{FeC} value. Finally, as also observed for the native protein system,¹³ the low-frequency shift of the δ_{FeCO} value with increasing number of CF₃ substitutions suggested that the orientation of the Fe-bound CO, with respect to the heme, in the mutant protein is affected by the ρ_{Fe} value.

Vibrational Frequencies of Fe-Bound O₂ of the H64L Mutant and Native Proteins. Resonance Raman spectra of the O₂ forms of the mutant and native proteins (MbO₂ and H64LO₂, respectively) possessing various heme cofactors were obtained in order to determine the vibrational frequencies of the Fe–O stretching (ν_{FeO}) of Fe-bound O₂ in the proteins (Figure 4). The ν_{FeO} bands of the proteins were each observed as a single component, and the determined ν_{FeO} values are given in Table 2. The ν_{FeO} values of 571 and 569 cm⁻¹ determined for MbO₂(Proto) and H64LO₂(Proto), respectively, were similar to the corresponding values previously reported by Hirota et al.,²⁶ i.e., 571 and 570 cm⁻¹, for the former and latter, respectively. In contrast to the large mutation-dependent changes in the ν_{CO} and ν_{FeC} values (see above), the ν_{FeO} value was affected only slightly by the mutation. Comparison of the ν_{FeO} values among the mutant (or native) proteins, revealed that, although its effect is rather small, the ν_{FeO} value was decreased by the CF₃ substitutions, suggesting that the Fe²⁺–O bond in the protein is slightly weakened by the CF₃ substitutions. Hence, the weakening of the Fe²⁺–O bond in the protein with decreasing ρ_{Fe} value could be, in part, responsible for the decrease in the O₂ affinity of the protein induced by the CF₃ substitutions.

DISCUSSION

Correlation between the ν_{CO} and ρ_{Fe} Values of the H64L Mutant Protein. We have previously shown that the ν_{CO} value can be used as a sensitive measure of the ρ_{Fe} value.¹³ The relationship between the ν_{CO} and ρ_{Fe} values could be reasonably explained on the basis of the resonance between the two canonical forms of the Fe²⁺–CO fragment, represented by the valence bond formalism (Scheme 2).⁴⁴ The larger the ρ_{Fe} value, the better the heme Fe atom can serve as a π donor to CO. The stronger the Fe²⁺–CO bond, the greater will be the bond order of the Fe²⁺–CO bond, the smaller the C–O bond order, and hence the weaker the C–O bond. Consequently, the strength of the Fe²⁺–CO and C–O bonds increases and decreases, respectively, with increasing ρ_{Fe} value. As a result, a reciprocal relationship holds between the ν_{FeC} and ν_{CO} values, as has been demonstrated previously for the native proteins.⁴⁵ A similar $\nu_{\text{FeC}}-\nu_{\text{CO}}$ reciprocal relationship was observed for the mutant proteins examined in this study. This finding indicated that the effect of the in-plane electronic perturbation of the heme π system induced through heme cofactor modifications on the π back-donation of the heme Fe atom to CO is independent of the mutations.

As in the case of the native proteins,¹³ an additive effect of the heme π system perturbation induced by the CF₃ substitutions on the ν_{CO} value was observed for the mutant proteins. In fact, plots of the ν_{CO} values of the mutant proteins against the $\nu_{\text{CO(H)}}$ values of the native proteins can be represented by a straight line with a slope of 1 (see Figure S4 in the Supporting Information). This finding supported that changes in the ρ_{Fe} value due to the CF₃ substitutions are independent of the H64L mutation.

In contrast to the case of the ν_{CO} value, the change in the ν_{FeC} value of the mutant protein due to the heme π system perturbation induced by the CF₃ substitutions could not be simply interpreted in terms of the ρ_{Fe} value. Considering the

ν_{FeC} values of the native proteins, which ranged only over 3 cm^{-1} , the ν_{FeC} value of H64LCO(2,8-DPF) is anomalously smaller in comparison with those of the other mutant proteins: i.e., 484 cm^{-1} for H64LCO(2,8-DPF) and $490\text{--}493 \text{ cm}^{-1}$ for the other H64L mutant proteins. Similarly, H64LCO(2,8-DPF) also exhibited a δ_{FeCO} value slightly different from those of the other mutant proteins: i.e., 570 and $573\text{--}575 \text{ cm}^{-1}$ for the former and latter, respectively. This result suggested that the orientation of the Fe-bound CO with respect to the heme plane in H64LCO(2,8-DPF) is slightly different from those in the other mutant proteins. Hence, the absence of a simple relationship between the ν_{FeC} value and the heme cofactor modifications for the mutant proteins could be due to the altered Fe–CO conformation in H64LCO(2,8-DPF).

Effect of a Change in the ρ_{Fe} Value on the Fe–O Bond in O_2 Forms of the Proteins. As shown in Table 2, the ν_{FeO} value of the native protein was slightly affected by the H64L mutation. An $\text{Fe}^{3+}\text{--O}_2^-$ -like species has been expected for the $\text{Fe}^{2+}\text{--O}_2$ bond in the O_2 form of a protein (Scheme 1).^{20,21} Although the resonance between the two alternative structures of the Fe– O_2 fragment is thought to be affected by the heme environment furnished by nearby amino acid residues and the heme electronic structure, the Fe–O bond order is independent of the resonance. Consequently, the relatively low sensitivity of the ν_{FeO} value to replacement of amino acid residues in the heme pocket has been attributed to the fixed Fe–O bond order.²⁶ Comparison of the ν_{FeO} values among the mutant (or native) proteins possessing various heme cofactors demonstrated that the ν_{FeO} value decreases steadily with increasing number of CF_3 substitutions, although the differences are quite small. This finding indicated that the Fe–O bond in the Fe– O_2 fragment is weakened by the CF_3 substitutions, possibly owing to the hindrance of the formation of an $\text{Fe}^{3+}\text{--O}_2^-$ -like species through obstruction of the Fe–O bond polarization by the decreasing ρ_{Fe} value due to the CF_3 substitutions. This finding also supported the idea proposed by Pauling²⁰ that the Fe–O bond strength is affected by the electronic nature of the bond.

Electronic Control of CO Affinity of the H64L Mutant Protein. The $k_{\text{off}}(\text{CO})$ values of the mutant proteins exhibited CF_3 -substitution-dependent changes such that the values of H64LCO(7-PF) and H64LCO(2,8-DPF) were $\sim 1/4$ to $\sim 1/5$ of those of the corresponding counterparts, i.e., H64LCO(Meso) and H64LCO(3,8-DMD), respectively, although their $k_{\text{on}}(\text{CO})$ values were similar to each other (Table 2). The results for the mutant proteins were different from those for the native proteins, demonstrating that not only the $k_{\text{on}}(\text{CO})$ value but also the $k_{\text{off}}(\text{CO})$ value was essentially independent of the heme cofactor modifications. The heme cofactor dependent changes of the $k_{\text{off}}(\text{CO})$ value of the mutant protein could be interpreted in terms of the stabilities of the canonical structures of the Fe–CO fragment associated with an electrostatic interaction between partial charges of the Fe-bound CO and nearby amino acid side chains (Scheme 2). The distal His64 provides a positive electrostatic potential near the terminal O atom of the Fe-bound CO and, due to the electrostatic interaction between the His64 and Fe-bound CO, structure II in Scheme 2 prevails over structure I.²⁴ On the other hand, in the case of the H64L mutant, the stability of the Fe–CO bond is predominantly affected by the electronic nature of the heme cofactor. The coordination of CO to the heme Fe atom is thought to result in an increase in the ρ_{Fe} value, due to the σ donation from CO to the heme Fe, which would lead to a

kinetic instability of the Fe–CO bond. The substitution of CF_3 group(s) is thought to moderate an increase in the ρ_{Fe} value upon the coordination of CO to the heme Fe atom, resulting in enhancement of the stability of the Fe–CO bond, as manifested in the observed $k_{\text{off}}(\text{CO})$ values (Table 1). Thus, the present results suggested that the $k_{\text{off}}(\text{CO})$ value of the mutant protein is determined by not only the electronic environment near the Fe-bound ligand but also the heme electronic structure. This interpretation was supported by the plots of the quantity $\log(K(\text{CO}))$ against the ν_{CO} values for the mutant proteins (Figure 5), which could be represented by a

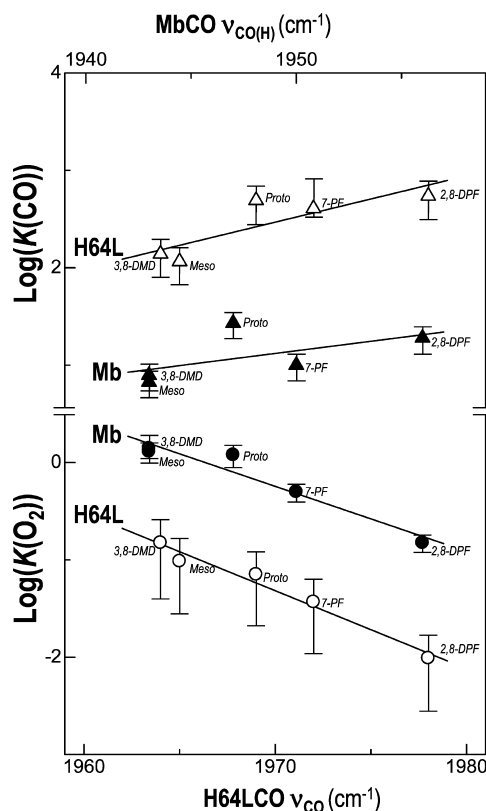


Figure 5. Plots of the quantities $\log(K(\text{O}_2))$ and $\log(K(\text{CO}))$ against the ν_{CO} and $\nu_{\text{CO(H)}}$ values for the H64L mutant and native proteins, respectively: (○) $\log(K(\text{O}_2))\text{--}\nu_{\text{CO}}$; (△) $\log(K(\text{CO}))\text{--}\nu_{\text{CO}}$; (●) $\log(K(\text{O}_2))\text{--}\nu_{\text{CO(H)}}$; (▲) $\log(K(\text{CO}))\text{--}\nu_{\text{CO(H)}}$. The lower and upper horizontal axes represent the ν_{CO} and $\nu_{\text{CO(H)}}$ values for the H64L mutant and native proteins, respectively, and are graduated in such a way that the mean ν_{CO} and $\nu_{\text{CO(H)}}$ values are at the center of the axes. The best-fitting straight lines were drawn for each set of the plots. The $\log(K(\text{CO}))\text{--}\nu_{\text{CO}}$, $\log(K(\text{O}_2))\text{--}\nu_{\text{CO}}$, and $\log(K(\text{CO}))\text{--}\nu_{\text{CO(H)}}$ plots could be represented by straight lines with slopes of ~ 0.05 , ~ -0.08 , and ~ -0.08 ($1/\text{cm}^{-1}$), respectively. Although the $\log(K(\text{CO}))\text{--}\nu_{\text{CO(H)}}$ plots also appeared to be represented by a straight line, the linear relationship between the $\log(K(\text{CO}))$ and $\nu_{\text{CO(H)}}$ values of the protein could not be supported by the $\log(k_{\text{on}}(\text{CO}))\text{--}\nu_{\text{CO(H)}}$ and $\log(k_{\text{off}}(\text{CO}))\text{--}\nu_{\text{CO(H)}}$ plots (Table 1; see also Figures S5 and S6 in the Supporting Information).

straight line with a slope of ~ 0.05 ($1/\text{cm}^{-1}$). The large deviation of the plot for H64L(2,8-DPF) from the straight line could be due to its altered Fe–CO conformation, as reflected in its δ_{FeCO} value (see above).

Electronic Control of O_2 Affinity of the H64L Mutant Protein. We have shown previously that the O_2 affinity of a native protein is regulated by the ρ_{Fe} value in such a manner

that the O_2 affinity of the protein decreases, due to an increase in the $k_{\text{off}}(O_2)$ value, with a decrease in the ρ_{Fe} value.^{11,13} The O_2 binding parameters in Table 1 demonstrate that the O_2 affinity of the H64L mutant protein is controlled in a similar manner. In order to characterize the relationship between the O_2 affinity and the ρ_{Fe} value in the mutant and native proteins, the $\log(K(O_2))-\nu_{\text{CO}}$ plots for the two different protein systems are compared with each other in Figure 5 (see also Figures S5 and S6 in the Supporting Information). The plots for the mutant and native proteins could be represented by straight lines with slopes of ~ -0.08 ($1/\text{cm}^{-1}$), suggesting that the effect of a change in the ρ_{Fe} value on the O_2 affinity is essentially independent of the removal of the distal His64 and, hence, the distal H bond. Furthermore, the Mb(3,8-DMD)/Mb(2,8-DPF) and H64L(3,8-DMD)/H64L(2,8-DPF) systems exhibited decreases in the $K(O_2)$ value by factors of ~ 9 and ~ 15 , respectively, on the substitution of two CF_3 groups. On the other hand, comparison between the mutant and native protein possessing identical heme cofactors indicated that the $K(O_2)$ value was decreased by a factor of ~ 9 to ~ 17 by the H64L mutation. Consequently, the decrease in the O_2 affinity of the protein through a decrease in the ρ_{Fe} value induced by the substitution of two CF_3 groups was found to be almost comparable to that due to the removal of the distal His64. Thus, in addition to the heme environment furnished by the His64,^{1,6} the electronic tuning of the intrinsic heme Fe reactivity through the ρ_{Fe} value was found to be a major determinant for control of the O_2 affinity of the protein.

Electronic Control of O_2 /CO Discrimination in the H64L Mutant Protein. The M value of the H64L mutant protein increased by factors of ~ 9 and ~ 60 on the substitution of one and two CF_3 groups, respectively, whereas that of the native protein increased by factors of only ~ 4 and ~ 25 on the substitution of one and two CF_3 groups, respectively.¹³ These results demonstrated that the distal His64 drastically diminishes the effect of a change in the ρ_{Fe} value on the M value. The $k_{\text{off}}(O_2)$ and $k_{\text{off}}(\text{CO})$ values of the mutant protein increased and decreased, respectively, with a decrease in the ρ_{Fe} value, whereas both the $k_{\text{on}}(O_2)$ and $k_{\text{on}}(\text{CO})$ values were almost independent of the ρ_{Fe} value. Hence, the remarkably large increase in the M value of the mutant protein induced by a decrease in the ρ_{Fe} value is due to the opposite ρ_{Fe} dependence of the O_2 and CO affinities: i.e., the former and latter decrease and increase with a decrease in the ρ_{Fe} value, respectively (see also Figures S7 and S8 in the Supporting Information). Thus, both the heme environment furnished by His64 and the electronic tuning of the intrinsic heme Fe reactivity through the ρ_{Fe} value contribute significantly to regulation of the protein function.

Understanding the mechanisms underlying the O_2 /CO discrimination in Mb is a problem of immense fundamental and practical importance. Respiratory proteins have to exhibit considerably small M values in order to perform their biological activities in the presence of low levels of CO. The M value of Mb(Proto): i.e., ~ 20 (Table 1), is $\sim 1/1000$ of those of simple heme Fe(II) model complexes, i.e., $\sim 2 \times 10^4$,^{8,10} and the dramatic reduction of the M value in the protein has been interpreted in terms of the heme environment furnished by nearby amino acid residues, particularly the distal His64. The ~ 1000 -fold decrease in the M value of the protein has been accounted for by a ~ 100 -fold increase in the O_2 affinity induced by stabilizing Fe(II)-bound O_2 through the distal H bond, together with a ~ 10 -fold decrease in the CO affinity possibly

due to unfavorable steric interaction of Fe-bound CO with His64 and other distal residues.² The present study demonstrated that, even in the absence of His64, the M value of the protein can be regulated solely through the ρ_{Fe} value. This finding provided novel insights into mechanisms underlying the O_2 /CO discrimination in the protein.

CONCLUSION

As in the case of the native protein, the O_2 affinity of the H64L mutant protein was found to be regulated by the ρ_{Fe} value in such a manner that the O_2 affinity of the protein decreases, due to an increase in the $k_{\text{off}}(O_2)$ value, with a decrease in the ρ_{Fe} value. On the other hand, we found that the CO affinity of the H64L mutant protein increases, due to a decrease in the $k_{\text{off}}(\text{CO})$ value, with a decrease in the ρ_{Fe} value, whereas that of the native protein was essentially independent of a change in the ρ_{Fe} value. As a result, the regulation of the O_2 /CO discrimination in Mb through the heme electronic structure is affected by the distal His64. These results not only demonstrated that the O_2 and CO affinities of Mb lacking the distal His64 can be controlled solely by the ρ_{Fe} value but also revealed a novel relationship between the regulation of the Mb function through the heme environment furnished by the distal His64 and that of electronic tuning of the intrinsic heme Fe reactivity through the ρ_{Fe} value. These findings provided crucial insights into the structure–function relationships in the protein.

ASSOCIATED CONTENT

Supporting Information

Figures S1–S8, as described in the text. This material is available free of charge via the Internet at <http://pubs.acs.org>.

AUTHOR INFORMATION

Corresponding Author

*Y.Y.: tel/fax, +81 29 853 6521; e-mail, yamamoto@chem.tsukuba.ac.jp.

Notes

The authors declare no competing financial interest.

ACKNOWLEDGMENTS

This work was supported by the Yazaki Memorial Foundation for Science and Technology and the NOVARTIS Foundation (Japan) for the Promotion of Science.

REFERENCES

- (1) Olson, J. S.; Mathews, A. J.; Rohlf, R. J.; Springer, B. A.; Egeberg, K. D.; Sligar, S. G.; Tame, J.; Renaud, J.-P.; Nagai, K. *Nature* **1988**, *336*, 265–266.
- (2) Kachalova, G. S.; Popov, A. N.; Bartunik, H. D. *Science* **1999**, *284*, 473–476.
- (3) Chu, K.; Vojtchovsky, J.; McMahon, B. H.; Sweet, R. M.; Berendzen, J.; Schlichting, I. *Nature* **2000**, *403*, 921–923.
- (4) Schotte, F.; Lim, M.; Jackson, T. A.; Smirnov, A. V.; Soman, J.; Olson, J. S.; Phillips, G. N., Jr.; Wulff, M.; Anfirud, P. A. *Science* **2003**, *300*, 1944–1947.
- (5) Antonini, E.; Brunori, M. *Hemoglobins and Myoglobins and their Reactions with Ligands*; North Holland: Amsterdam, 1971.
- (6) Springer, B. A.; Egeberg, K. D.; Sligar, S. G.; Rohlf, R. J.; Mathews, A. J.; Olson, J. S. *J. Biol. Chem.* **1989**, *264*, 3057–3060.
- (7) Springer, B. A.; Sligar, S. G.; Olson, J. S.; Phillips, G. N., Jr. *Chem. Rev.* **1994**, *94*, 699–714.
- (8) Olson, J. S.; Phillips, G. N., Jr. *J. Biol. Inorg. Chem.* **1997**, *2*, 544–552.

- (9) Capece, L.; Marti, M. A.; Crespo, A.; Doctorovich, F.; Estrin, D. A. *J. Am. Chem. Soc.* **2006**, *128*, 12455–12461.
- (10) Olson, J. S.; McKinnie, R. E.; Mims, M. P.; White, D. K. *J. Am. Chem. Soc.* **1983**, *105*, 1522–1527.
- (11) Shibata, T.; Nagao, S.; Fukaya, M.; Tai, H.; Nagatomo, S.; Morihashi, K.; Matsuo, T.; Hirota, S.; Suzuki, A.; Imai, K.; Yamamoto, Y. *J. Am. Chem. Soc.* **2010**, *132*, 6091–6098.
- (12) Shibata, T.; Matsumoto, D.; Nishimura, R.; Tai, H.; Matsuoka, A.; Nagao, S.; Matsuo, T.; Hirota, S.; Imai, K.; Neya, S.; Suzuki, A.; Yamamoto, Y. *Inorg. Chem.* **2012**, *51*, 11955–11960.
- (13) Nishimura, R.; Shibata, T.; Tai, H.; Ishigami, I.; Ogura, T.; Nagao, S.; Matsuo, T.; Hirota, S.; Imai, K.; Neya, S.; Suzuki, A.; Yamamoto, Y. *Inorg. Chem.* **2013**, *52*, 3349–3355.
- (14) Phillips, S. E. V.; Schoenborn, B. P. *Nature* **1981**, *292*, 81–82.
- (15) Kitagawa, T.; Ondrias, M. R.; Rousseau, D. L.; Ikeda-Saito, M.; Yonetani, T. *Nature* **1982**, *298*, 869–871.
- (16) Lukin, J. A.; Simplaceanu, V.; Zou, M.; Ho, N. T.; Ho, C. *Proc. Natl. Acad. Sci. U.S.A.* **2000**, *97*, 10354–10358.
- (17) Chang, C. K.; Ward, B.; Ebina, S. *Arch. Biochem. Biophys.* **1984**, *231*, 366–371.
- (18) Neya, S.; Suzuki, M.; Hoshino, T.; Ode, H.; Imai, K.; Komatsu, T.; Ikezaki, A.; Nakamura, M.; Furutani, Y.; Kandori, H. *Biochemistry* **2010**, *49*, 5642–5650.
- (19) Toi, H.; Homma, M.; Suzuki, A.; Ogoshi, H. *J. Chem. Soc., Chem. Commun.* **1985**, 1791–1792.
- (20) Pauling, L. *Nature* **1964**, *203*, 182–183.
- (21) Maxwell, J. C.; Volpe, J. A.; Barlow, C. H.; Caughey, W. S. *Biochem. Biophys. Res. Commun.* **1974**, *58*, 166–171.
- (22) Quillin, M. L.; Arduini, R. M.; Olson, J. S.; Phillips, G. N., Jr. *J. Mol. Biol.* **1993**, *234*, 140–155.
- (23) Sakan, Y.; Ogura, T.; Kitagawa, T.; Fraunfelder, F. A.; Mattera, R.; Ikeda-Saito, M. *Biochemistry* **1993**, *32*, 5815–5824.
- (24) Li, T.; Quillin, M. L.; Phillips, G. N., Jr.; Olson, J. S. *Biochemistry* **1994**, *33*, 1433–1446.
- (25) Anderton, C. L.; Hester, R. E.; Moore, J. N. *Biochim. Biophys. Acta* **1997**, *1338*, 107–120.
- (26) Hirota, S.; Li, T.; Phillips, G. N., Jr.; Olson, J. S.; Mukai, M.; Kitagawa, T. *J. Am. Chem. Soc.* **1996**, *118*, 7845–7846.
- (27) Birukou, I.; Schweers, R. L.; Olson, J. S. *J. Biol. Chem.* **2010**, *285*, 8840–8854.
- (28) Teale, F. W. J. *Biochim. Biophys. Acta* **1959**, *35*, 543.
- (29) Imai, K. *Methods Enzymol.* **1981**, *76*, 438–449.
- (30) Imai, K. *Methods Enzymol.* **1981**, *76*, 470–486.
- (31) Olson, J. S. *Method. Enzymol.* **1981**, *76*, 631–651.
- (32) Rohlfs, R. J.; Mathews, A. J.; Carver, T. E.; Olson, J. S.; Springer, B. A.; Egeberg, K. D.; Sliger, S. G. *J. Biol. Chem.* **1990**, *265*, 3168–3176.
- (33) Hayashi, T.; Dejima, H.; Matsuo, T.; Sato, H.; Murata, D.; Hisaeda, Y. *J. Am. Chem. Soc.* **2002**, *124*, 11226–11227.
- (34) Matsuo, T.; Dejima, H.; Hirota, S.; Murata, D.; Sato, H.; Ikegami, T.; Hori, H.; Hisaeda, Y.; Hayashi, T. *J. Am. Chem. Soc.* **2004**, *126*, 16007–16017.
- (35) Matsuo, T.; Ikegami, T.; Sato, H.; Hisaeda, Y.; Hayashi, T. *J. Inorg. Biochem.* **2006**, *100*, 1265–1271.
- (36) Kitanishi, K.; Kobayashi, K.; Kawamura, Y.; Ishigami, I.; Ogura, T.; Nakajima, K.; Igarashi, J.; Tanaka, A.; Shimizu, T. *Biochemistry* **2010**, *49*, 10381–10393.
- (37) Reilly, J. T.; Walsh, J. M.; Greenfield, M. L.; Donohue, M. D. *Spectrochim. Acta* **1992**, *48A*, 1459–1479.
- (38) La Mar, G. N.; Satterlee, J. D.; de Ropp, J. S. In *The Porphyrin Handbook*; Kadish, K., Smith, K. M., Guillard, R., Eds.; Academic Press: New York, 2000; pp 185–298.
- (39) Bertini, I.; Luchinat, C. *NMR of Paramagnetic Molecules in Biological Systems*; Benjamin/Cummings: Menlo Park, CA, 1986; pp 19–46.
- (40) Yamamoto, Y. *Annu. Rep. NMR Spectrosc.* **1998**, *36*, 1–77.
- (41) Ramaprasad, S.; Johnson, R. D.; La Mar, G. N. *J. Am. Chem. Soc.* **1984**, *106*, 5330–5335.
- (42) Emerson, S. D.; La Mar, G. N. *Biochemistry* **1990**, *29*, 1545–1556.
- (43) La Mar, G. N.; Budd, D. L.; Viscio, D. B.; Smith, K. M.; Langry, L. C. *Proc. Natl. Acad. Sci. U.S.A.* **1978**, *75*, 5755–5759.
- (44) Alben, J. O.; Caughey, W. S. *Biochemistry* **1968**, *7*, 175–183.
- (45) Li, X.-Y.; Spiro, T. G. *J. Am. Chem. Soc.* **1988**, *110*, 6024–6033.
- (46) Tsubaki, M.; Srivastava, R. B.; Yu, N. T. *Biochemistry* **1982**, *21*, 1132–1140.